

# Nuclear Medium Effects on the Structure Functions

Sergey Kulagin

Institute for Nuclear Research of the Russian Academy of Sciences, Moscow

Talk at the  
*SIS/DIS Workshop*

Gran Sasso Science Institute, L'Aquila, Italy  
October 11-13, 2018

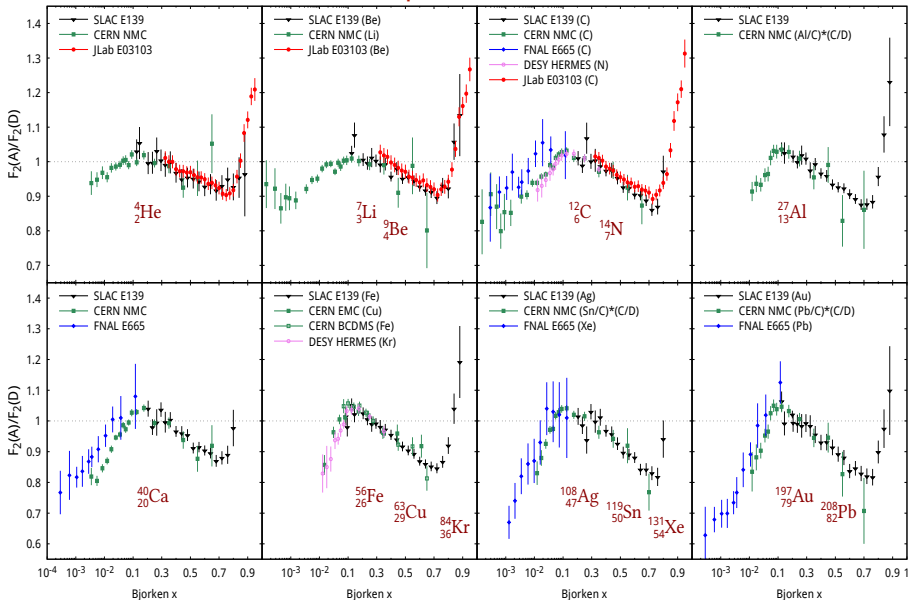
# Outline

- ▶ Experimental observations on modification of partonic structure of nuclei
- ▶ Understanding and modelling nuclear corrections in DIS region
  - ▶ Sketch of basic mechanisms of nuclear DIS in different kinematic regions.
  - ▶ Brief review of our efforts to build a quantitative model of nuclear structure functions.
- ▶ Extend the model into the resonance region. Discuss the ratios  $D/(p+n)$  and  ${}^3\text{He}/D$  and  ${}^3\text{He}/(D+p)$  in comparison with JLab *BONuS, 2015* and *Hall C, 2009* measurements.
- ▶ Summary/Conclusions

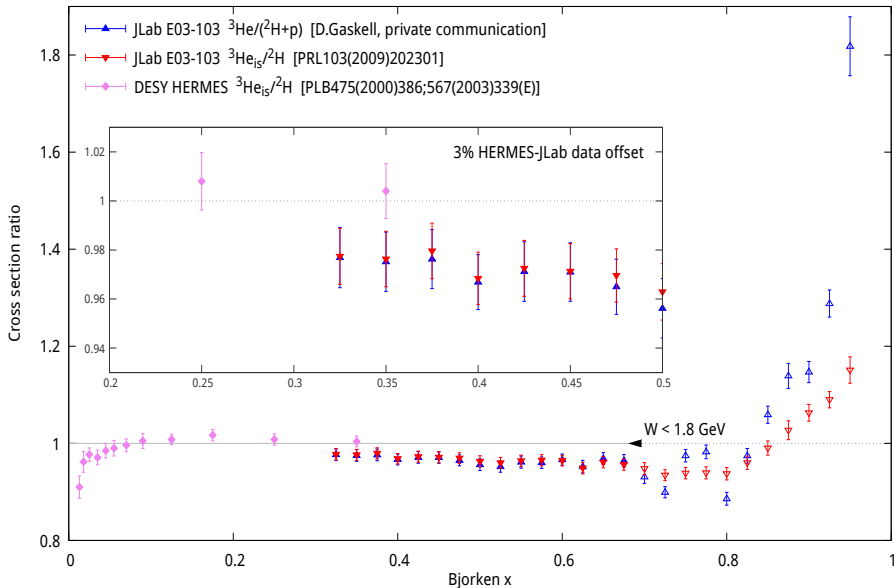
# Data summary on nuclear effects on the parton level

- ▶ Nuclear ratios  $\mathcal{R}(A/B) = \sigma_A(x, Q^2)/\sigma_B(x, Q^2)$  or  $F_2^A/F_2^B$  from DIS experiments
- ▶ Data for nuclear targets from  ${}^2\text{H}$  to  ${}^{208}\text{Pb}$ 
  - ▶ Fixed-target experiments with  $e/\mu$ :
    - ▶ Muon beam at CERN (EMC, BCDMS, NMC) and FNAL (E665).
    - ▶ Electron beam at SLAC (E139, E140), HERA (HERMES), JLab (E03-103).
  - ▶ Kinematics and statistics:  
Data covers the region  $10^{-4} < x < 1.5$  and  $0 < Q^2 < 150 \text{ GeV}^2$ . About 800 data points for the nuclear ratios  $\mathcal{R}(A/B)$  with  $Q^2 > 1 \text{ GeV}^2$ .
- ▶ Nuclear effects for antiquarks have been probed by Drell-Yan experiments at FNAL (E772, E866).
- ▶ Nuclear cross sections from high-energy measurements with neutrino BEBC ( ${}^2\text{H}$  and  ${}^{20}\text{Ne}$ ), NOMAD ( ${}^{12}\text{C}$  and  ${}^{56}\text{Fe}$ ) CDHS, CCFR and NuTeV ( ${}^{56}\text{Fe}$ ) CHORUS ( ${}^{207}\text{Pb}$ ). Nuclear cross section ratios  $\text{Fe}/\text{CH}$  and  $\text{Fe}/\text{CH}$  from MINERvA in the region of low  $Q^2$ .

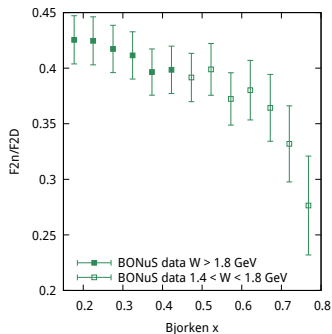
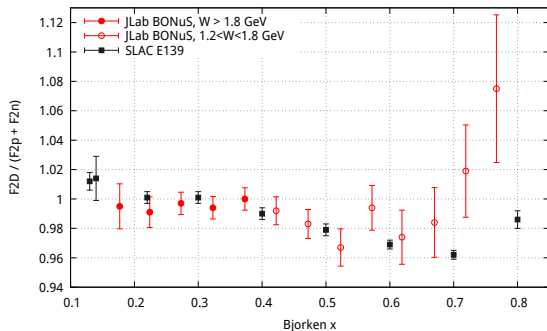
# Nuclear ratios from DIS experiments



# HERMES and JLab measurements on $^3\text{He}$



# SLAC E139 and JLab BONuS results on ${}^2\text{H}$



- ▶ SLAC E139 [[PRD49\(1994\)4348](#)] obtains  $R_D = F_2^D / (F_2^p + F_2^n)$  by extrapolating data on  $R_A = F_2^A / F_2^D$  with  $A \geq 4$  assuming  $R_A - 1$  scales as nuclear density.
- ▶ BONuS [[PRC92\(2015\)015211](#)] obtains  $R_D$  from a direct measurement of  $F_2^n / F_2^D$  [[PRC89\(2014\)045206](#)] using “world data” on  $F_2^D / F_2^p$ .

# Why nuclear corrections survive at DIS?

Space-time scales in DIS

$$W_{\mu\nu} = \int d^4x \exp(iq \cdot x) \langle p | [J_\mu(x), J_\nu(0)] | p \rangle$$

$$q \cdot x = q_0 t - |\mathbf{q}|z = q_0 t - \sqrt{q_0^2 + Q^2}z \simeq q_0(t - z) - \frac{Q^2}{2q_0} z$$

- ▶ DIS proceeds near the light cone:  $|t - z| \sim 1/q_0$  and  $t^2 - z^2 \sim Q^{-2}$ .
- ▶ In the TARGET REST frame the characteristic time and longitudinal distance are NOT small at all:  $t \sim z \sim 2q_0/Q^2 = 1/Mx_{\text{Bj}}$ . DIS proceeds at the distance  $\sim 1$  Fm at  $x_{\text{Bj}} \sim 0.2$  and at the distance  $\sim 20$  Fm at  $x_{\text{Bj}} \sim 0.01$ .
- ▶ Two different regions in nuclei from comparison of coherence length (loffe time)  $L = 1/Mx_{\text{Bj}}$  with average distance between bound nucleons  $r_{\text{NN}}$ :
  - ▶  $L < r_{\text{NN}}$  (or  $x > 0.2$ )  $\Rightarrow$  Nuclear DIS  $\approx$  incoherent sum of contributions from bound nucleons. Nuclear corrections  $\sim EL$  and  $\sim |\mathbf{p}|^2 L^2$  where  $E(\mathbf{p})$  typical energy (momentum) in the nuclear ground state.
  - ▶  $L \gg r_{\text{NN}}$  (or  $x \ll 0.2$ )  $\Rightarrow$  Coherent effects of interactions with a few nucleons are important.





## Nuclear spectral function

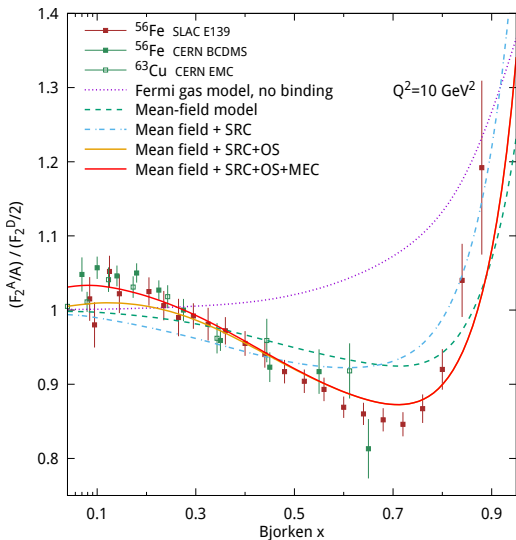
The nuclear spectral function describes probability to find a bound nucleon with momentum  $\mathbf{p}$  and energy  $p_0 = M + \varepsilon$ :

$$\begin{aligned}\mathcal{P}(\varepsilon, \mathbf{p}) &= \int dt e^{-i\varepsilon t} \langle \psi^\dagger(\mathbf{p}, t) \psi(\mathbf{p}, 0) \rangle \\ &= \sum_i |\langle (A-1)_i, -\mathbf{p} | \psi(0) | A \rangle|^2 2\pi \delta(\varepsilon + E_i^{A-1}(\mathbf{p}) - E_0^A)\end{aligned}$$

- ▶ The sum runs over all possible states of the spectrum of  $A - 1$  residual system.
- ▶ The nuclear spectral function determines the rate of nucleon removal reactions such as  $(e, e'p)$ . For low separation energies and momenta,  $|\varepsilon| < 50 \text{ MeV}$ ,  $p < 250 \text{ MeV}/c$ , the observed spectrum is dominated by bound states  $A - 1$  similar to those predicted by the mean-field model.
- ▶ High-energy and high-momentum components of nuclear spectrum is not described by the mean-field model and driven by correlation effects in nuclear ground state (short-range correlations, or SRC). We combine the mean-field together with SRC contributions and consider a two-component model  $\mathcal{P} = \mathcal{P}_{\text{MF}} + \mathcal{P}_{\text{cor}}$  *Ciofi degli Atti & Simula, 1995 S.K. & Sidorov, 2000 S.K. & Petti, 2004*

# EMC effect in impulse approximation (IA)

- ▶ Impulse approximation:  
 $F_2(x', Q^2, p^2) = F_2(x', Q^2, M^2)$
- ▶ Momentum distribution (Fermi motion) leads to a rise at large Bjorken  $x$  *Atwood & West, 1970s*.
- ▶ Nuclear binding correction is important and results in a “dip” at  $x \sim 0.6 - 0.7$   
*Akulonichev, Vagradoy & S.K., 1984*.
- ▶ However, even realistic nuclear spectral function fails to accurately explain the slope and the position of the minimum in IA. Corrections to IA are needed!



## Nucleon off-shell effect (OS)

Bound nucleons are off-mass-shell,  $p^2 < M^2$ . The treatment of  $p^2$  dependence can greatly be simplified in the vicinity of the mass shell. If the virtuality parameter  $v = (p^2 - M^2)/M^2$  is small (e.g. average virtuality  $v \sim -0.15$  for  $^{56}\text{Fe}$ ) then expand  $q(x, Q^2, p^2)$  in series in  $v$

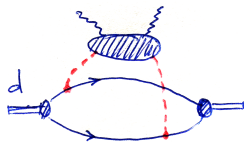
$$F_2^N(x, Q^2, p^2) \approx F_2^N(x, Q^2) (1 + \delta f(x, Q^2) v)$$

- ▶  $\delta f(x, Q^2)$  is a special structure function describing the modification of the off-shell nucleon PDFs in the vicinity of the mass shell.
- ▶ Off-shell correction is closely related to modification of the nucleon size in nuclear environment *S.K. & R.Petti, 2004.*

## Nuclear meson-exchange current effect (MEC)

Leptons can scatter on nuclear meson field which mediate interaction between bound nucleons. This process generate a MEC correction to nuclear sea quark distribution

$$\delta F_2^{\text{MEC}}(x, Q^2) = \int_x dy f_{\pi/A}(y) F_2^{\pi}(\frac{x}{y}, Q^2)$$

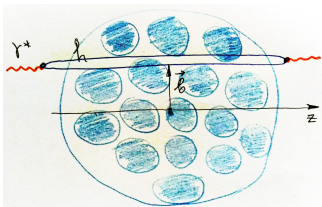


- ▶ Contribution from nuclear pions (mesons) is important to balance nuclear light-cone momentum  $\langle y \rangle_{\pi} + \langle y \rangle_N = 1$ .
- ▶ The nuclear pion distribution function is localized in a region  $y < p_F/M \sim 0.3$ . For this reason the MEC correction to nuclear (anti)quark distributions is localized at  $x < 0.3$ .
- ▶ The magnitude of the correction is driven by average number of “nuclear pion excess”  $n_{\pi} = \int dy f_{\pi/A}(y)$  and  $n_{\pi}/A \sim 0.1$  for a heavy nucleus like  $^{56}\text{Fe}$ .

## Nuclear shadowing

Coherent nuclear correction is due to propagation of intermediate state  $\gamma^* \rightarrow h$  in nuclear environment, which can be described in the multiple scattering theory

*Glauber, Gribov 1970s.*



$$\frac{\delta F_{2A}^{\text{coh}}}{F_{2N}} = \frac{\text{Im } \delta \mathcal{A}}{\text{Im } a}$$

$$\delta \mathcal{A} = \delta \mathcal{A}^{(2)} + \delta \mathcal{A}^{(3)} + \dots$$

$$\delta \mathcal{A}^{(2)} = ia^2 \int_{z_1 < z_2} d^2 \mathbf{b} dz_1 dz_2 \rho(\mathbf{b}, z_1) \rho(\mathbf{b}, z_2) e^{i \frac{z_1 - z_2}{L}}$$

- ▶  $\rho(\mathbf{r})$  is the nuclear number density,  $\int d^3 \mathbf{r} \rho(\mathbf{r}) = A$
- ▶  $a = \frac{\sigma}{2}(i + \alpha)$  is the (effective) forward scattering amplitude of intermediate state  $h$  off the nucleon
- ▶  $L$  is the coherence length of intermediate state which accounts finite life time of intermediate state,  $1/L = Mx(1 + m_h^2/Q^2)$ . Its presence suppresses the coherence effect in the region of large  $x$ .

# Modelling the nuclear corrections

Assemble everything together and confront model to data

*S.K. & R.Petti, NPA765(2006)126; PRC82(2010)054614; PRC90(2014)045204*

$$F_2^A = Z \langle F_2^p \rangle + N \langle F_2^n \rangle + \delta F_2^{\text{MEC}} + \delta F_2^{\text{coh}}$$

Strategy of the analysis:

- ▶ Compute the proton and neutron structure functions in terms of free proton PDF with relevant perturbative QCD corrections, TMC, as well as HT correction.
- ▶ Using  $F_2^{p,n}$  compute nuclear structure functions/cross sections with accurate treatment of nuclear spectral function effects (Fermi-motion and nuclear binding), MEC and nuclear shadowing correction.
- ▶ Treat the off-shell function  $\delta f(x)$  and effective amplitude  $a$  as unknown and parametrize them. Study the data on the nuclear DIS in terms of the ratios  $F_2^A/F_2^B$  and determine  $\delta f(x)$  together with the amplitude  $a$  from data.
- ▶ Use the normalization conditions and the DIS sum rules (GLS, Adler) to determine the amplitude  $a$  (responsible for nuclear shadowing) in the region of high  $Q^2$ , which is not constrained by data.
- ▶ Verify the model by comparing the calculations with data not used in analysis.

# Structure functions in the DIS region

If  $Q^2$  is large compared the nucleon mass, the operator product expansion in QCD produces power series:

$$F_2(x, Q^2) = F_2^{LT, TMC}(x, Q^2) + \frac{H_2(x, Q)}{Q^2} + \dots$$

The leading term is given in terms of PDFs convoluted with coefficient functions:

$$F_2^{LT} = \left[ 1 + \frac{\alpha_S}{2\pi} C_q^{(1)} \right] \otimes x \sum_q e_q^2 (q + \bar{q}) \\ + \frac{\alpha_S}{2\pi} C_g^{(1)} \otimes xg + \mathcal{O}(\alpha_S^2)$$

The HT terms involve interaction between quarks and gluons and lack simple probabilistic interpretation. In the region of high Bjorken  $x$  and/or low  $Q^2$  (small  $W^2$ ) one has to account for the target mass correction *Georgi & Politzer, 1976*

$$F_2^{LT, TMC}(x, Q^2) = \frac{x^2}{\xi^2 \gamma^2} F_2^{LT}(\xi, Q^2) + \frac{6x^3 M^2}{Q^2 \gamma^4} \int_{\xi}^1 \frac{dz}{z^2} F_2^{LT}(z, Q^2) + \mathcal{O}(Q^{-4})$$

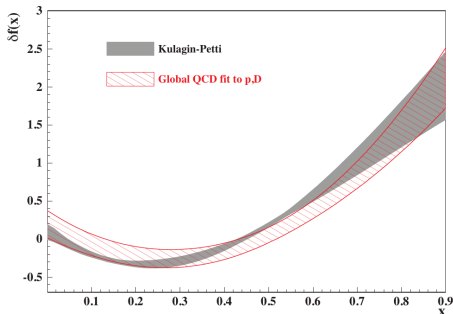
$\xi = 2x/(1 + \gamma)$  is the Nachtmann variable and  $\gamma^2 = 1 + 4x^2 M^2/Q^2$ . In this work we use the results of the PDF global analysis performed to QCD NNLO approximation (i.e. to order  $\alpha_S^2$ ) and which includes the proton (and deuteron) data sets from DIS, DY and collider data. Kinematical range  $0.8 < Q^2 < 10^5 \text{ GeV}^2$  and  $10^{-6} < x < 1$  with the cut  $W > 1.8 \text{ GeV}$  *S.Alekhin, K.Melnikov, F.Petriello, 2007; S.Alekhin, S.K., R.Petti, 2007*

# Determination of the off-shell function $\delta f(x)$

- ▶ Analysis of  $A/D$  and  $A/C$  ratios with a model

$\delta f(x) = C_N(x-x_1)(x-x_0)(1+x_0-x)$   
gives a good fit to all studied nuclei  
from  ${}^4\text{He}$  to  ${}^{208}\text{Pb}$  with  
 $\chi^2/\text{d.o.f.} = 459/556$  *S.K. & R.Petti, 2006.*

- ▶ A different approach: global QCD analysis using deuteron data and a model  $\delta f(x) = Ax^2 + Bx + C$  *Alekhin, S.K., Petti, 2017.*



- ▶ The function  $\delta f(x)$  provides a measure of the modification of the quark distributions in a bound nucleon.
- ▶ The slope of  $\delta f(x)$  in a single-scale nucleon model is related to the change of the radius of the nucleon in the nuclear environment *S.K. & R.Petti, 2006.* The observed slope suggests an increase in the bound nucleon radius in the iron by about 10% and in the deuteron by about 2%.



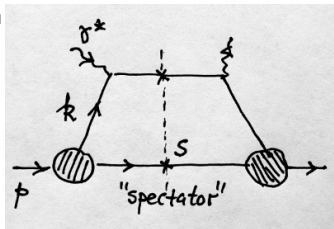
# Off-shell effect and the modification of the bound nucleon radius

The valence quark distribution in a (off-shell) nucleon

*Kulagin, Piller & Weise, PRC50(1994)1154*

$$q_{\text{val}}(x, p^2) = \int^{k_{\text{max}}^2} dk^2 \Phi(k^2, p^2)$$

$$k_{\text{max}}^2 = x(p^2 - s/(1-x))$$



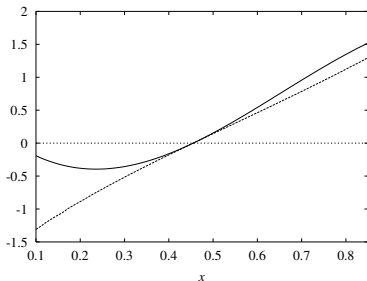
- ▶ A one-scale model of quark  $k^2$  distribution:  $\Phi(k^2) = C\phi(k^2/\Lambda^2)/\Lambda^2$ , where  $C$  and  $\phi$  are dimensionless and  $\Lambda$  is the scale.
- ▶ Off-shell:  $C \rightarrow C(p^2)$ ,  $\Lambda \rightarrow \Lambda(p^2)$
- ▶ The derivatives  $\partial_x q_{\text{val}}$  and  $\partial_{p^2} q_{\text{val}}$  are related

$$\delta f(x) = \frac{\partial \ln q_{\text{val}}}{\partial \ln p^2} = c + \frac{dq_{\text{val}}(x)}{dx} x(1-x)h(x)$$

$$h(x) = \frac{(1-\lambda)(1-x) + \lambda s/M^2}{(1-x)^2 - s/M^2}$$

$$c = \frac{\partial \ln C}{\partial \ln p^2}, \quad \lambda = \frac{\partial \ln \Lambda^2}{\partial \ln p^2}$$

- ▶ A simple pole model  $\phi(y) = (1 - y)^{-n}$  (note that  $y < 0$  so we do not run into singularity) provides a reasonable description of the nucleon valence distribution for  $x > 0.2$  and large  $Q^2$  ( $s = 2.1 \text{ GeV}^2$ ,  $\Lambda^2 = 1.2 \text{ GeV}^2$ ,  $n = 4.4$  at  $Q^2 = 15 \div 30 \text{ GeV}^2$ ).
- ▶ The size of the valence quark confinement region  $R_c \sim \Lambda^{-1}$  (nucleon core radius).
- ▶ Off-shell corection is independent of specific choice of profile  $\phi(y)$  and is given by  $(\ln q_{\text{val}}(x))'$ .
- ▶ Fix  $c$  and  $\lambda$  to reproduce  $\delta f(x_0) = 0$  and the slope  $\delta f'(x_0)$ . We obtain  $\lambda \approx 1$  and  $c \approx -2.3$ . The positive parameter  $\lambda$  suggests decreasing the scale  $\Lambda$  in nuclear environment (swelling of a bound nucleon)



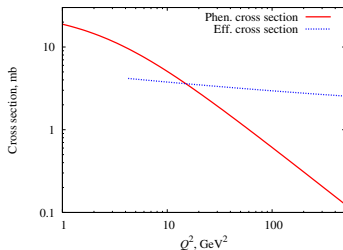
$$\frac{\delta R_c}{R_c} \sim -\frac{1}{2} \frac{\delta \Lambda^2}{\Lambda^2} = -\frac{1}{2} \lambda \frac{\langle p^2 - M^2 \rangle}{M^2}$$

$${}^{56}\text{Fe} : \delta R_c / R_c \sim 9\%$$

$${}^2\text{H} : \delta R_c / R_c \sim 2\%$$

# Determination of effective cross section

- ▶ The monopole form  $\sigma = \sigma_0 / (1 + Q^2 / Q_0^2)$  for the effective cross section of  $C$ -even  $q + \bar{q}$  combination provides a good fit to data on DIS nuclear shadowing for  $Q^2 < 15 \text{ GeV}^2$  with  $\sigma_0 = 27 \text{ mb}$  and  $Q_0^2 = 1.43 \pm 0.06 \pm 0.195 \text{ GeV}^2$ . Note  $\sigma_0$  is fixed from  $Q^2 \rightarrow 0$  limit by the vector meson dominance model. Also we assume  $\text{Re } a / \text{Im } a$  for  $C$ -even amplitude to be given by VMD at all energies.

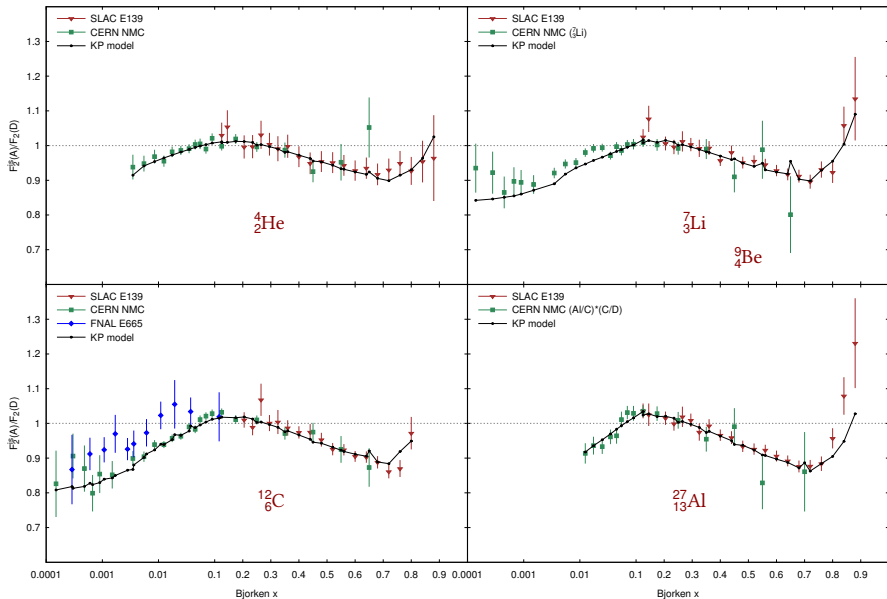


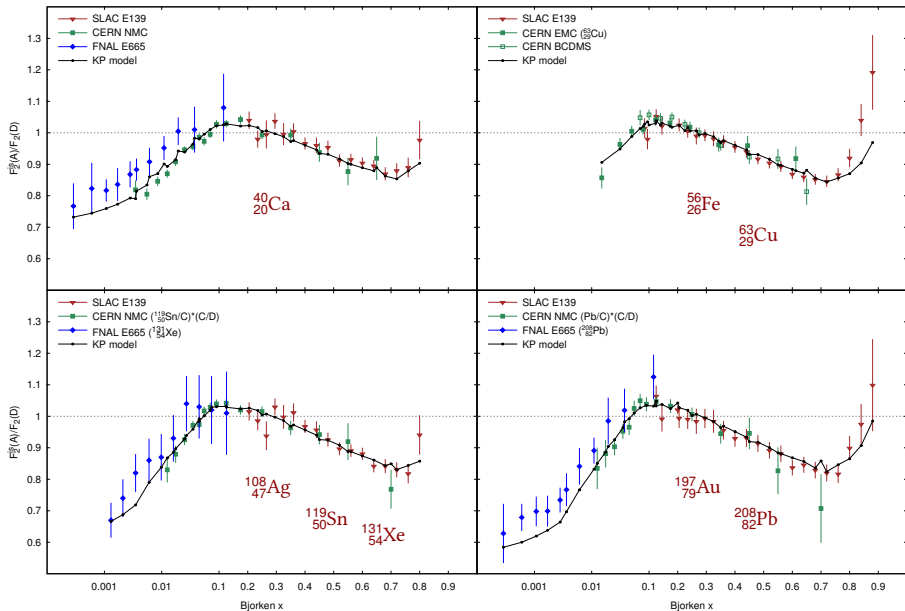
- ▶ Nuclear shadowing correction for the  $C$ -odd valence distribution  $q - \bar{q}$  is also driven by same cross section  $\sigma$ . Note, however, important interference effect between the phases of  $C$ -even and  $C$ -odd effective amplitude.
- ▶ The cross section at high  $Q^2 > 15 \text{ GeV}^2$  is not constrained by data. It is possible to evaluate  $\sigma$  in this region using the the normalization condition. Requiring exact cancellation between the off-shell and the shadowing correction in the normalization we have:

$$\int_0^1 dx \left( \langle v \rangle q_{\text{val}}(x, Q^2) \delta f(x) + \delta q_{\text{val}}^{\text{coh}}(x, Q^2) \right) = 0$$

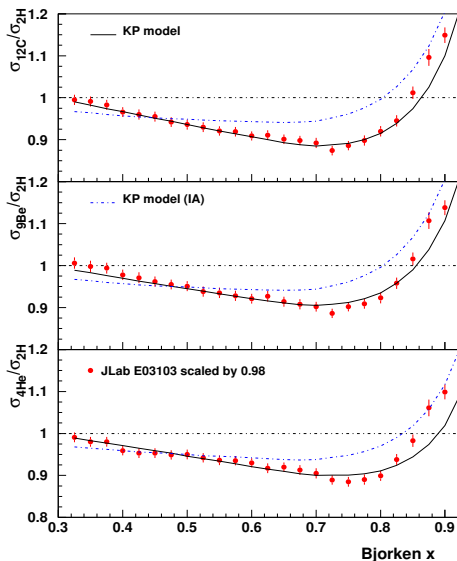
with  $\langle v \rangle = \langle p^2 - M^2 \rangle / M^2$  the average nucleon virtuality. Numeric solution to this equation is shown by dotted curve.

# Summary of results on the nuclear ratios $F_2^A/F_2^D$



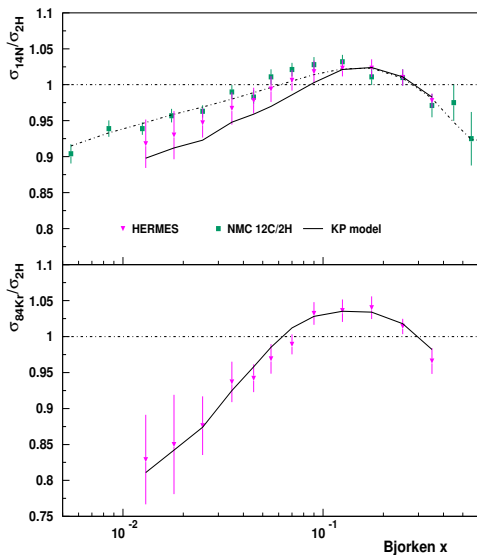


## Verification with recent JLab data (not a fit)



- ▶ Very good agreement of our predictions [S.K. & R.Petti, PRC82\(2010\)054614](#) with JLab E03-103 for all nuclear targets:  $\chi^2/d.o.f. = 26.3/60$  for  $W^2 > 2 \text{ GeV}^2$ .
- ▶ Nuclear corrections at large  $x$  is driven by nuclear spectral function, the off-shell function  $\delta f(x)$  was fixed from previous studies.
- ▶ A comparison with the Impulse Approximation (shown in blue) demonstrates that the off-shell correction is crucial to describe the data leading to both the modification of the slope and the position of the minimum of the ratios.

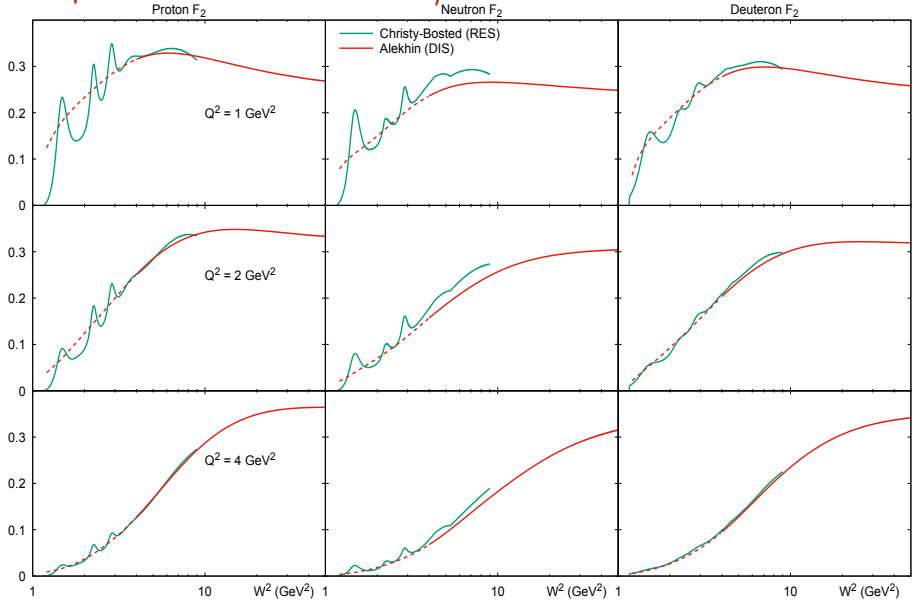
## Verification with HERMES data (not a fit)



- ▶ A good agreement of our predictions [S.K. & R.Petti, PRC82\(2010\)054614](#) with HERMES data for  $^{14}\text{N}/\text{D}$  and  $^{84}\text{Kr}/\text{D}$  with  $\chi^2/d.o.f. = 14.7/24$
- ▶ A comparison with CERN NMC data for  $^{12}\text{C}/\text{D}$  shows a notable  $Q^2$  dependence at small  $x$  in the shadowing region related to the  $Q^2$  dependence of effective cross-section.

The model correctly describes the observed  $x$  and  $Q^2$  dependence.

# Comparison of DIS and RES/SIS fits





# Duality

DIS and RES structure functions are dual in the integral sense *Bloom & Gilman, 1970*:

$$\int_{W_{\text{th}}^2}^{W_0^2} dW^2 F_2^{\text{DIS}}(W^2, Q^2) = \int_{W_{\text{th}}^2}^{W_0^2} dW^2 F_2^{\text{RES}}(W^2, Q^2)$$

$W_{\text{th}} = M_p + m_\pi$  the pion production threshold energy and  $W_0 = 2 \text{ GeV}$  the boundary of the resonance region.

Comparing Christy-Bosted (RES) and Alekhin (DIS) analyses:

- ▶ For the **proton** the error of the duality relation is better than 5% for  $1 \leq Q^2 < 10 \text{ GeV}^2$ .
- ▶ For the **neutron** the error is larger  $\sim 5 - 10\%$ . This could be related to a different treatment of the deuteron correction in Alekhin and CB fits.

## Hybrid model for the proton

A good matching between RES and DIS models in overlap region of  $1.8 < W < 3 \text{ GeV}$  motivates us to use a combined model in a wide region of  $W$  and  $Q^2$ :

$$F_2 = \begin{cases} F_2^{\text{RES}}(W^2), & W \leq W_1, \\ F_2^{\text{RES}}(W_1^2) + \frac{W^2 - W_1^2}{W_2^2 - W_1^2} (F_2^{\text{DIS}}(W_2^2) - F_2^{\text{RES}}(W_1^2)), & W_1 < W < W_2, \\ F_2^{\text{DIS}}(W^2), & W \geq W_2 \end{cases}$$

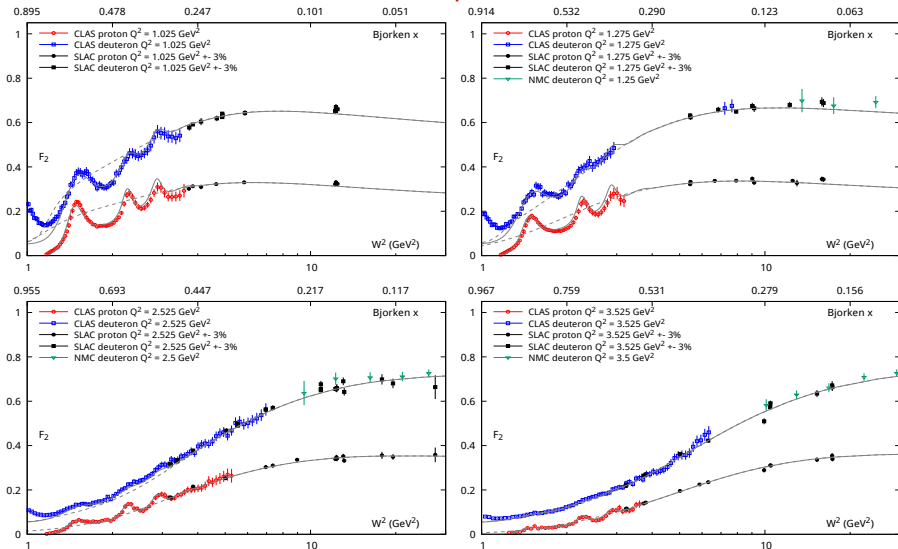
Here  $W_1 = 1.8 \text{ GeV}$  and  $W_2 = 2 \text{ GeV}$ .

## Hybrid model for the neutron

- ▶ For the neutron, the matching between RES and DIS models is somewhat worse than for the proton. As the neutron is extracted from the deuteron – proton difference, a significant part of disagreement could arise from a different treatment of the deuteron correction (discussed below).
- ▶ We compute neutron  $F_2^n$  in the resonance region using the RES model for the proton and the ratio  $R_{np} = F_2^n / F_2^p$  from the DIS model.
- ▶ Special care has to be taken in the  $\Delta(1232)$  region and near threshold. The isospin conservation suggests equal contribution to the proton and the neutron from the  $\Delta(1232)$  resonance =  $F_2^\Delta$  (supported by analysis *Bosted & Christy, 2010*).

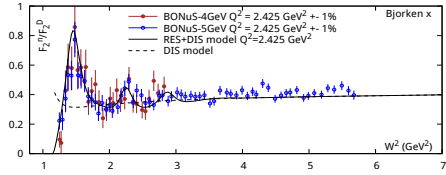
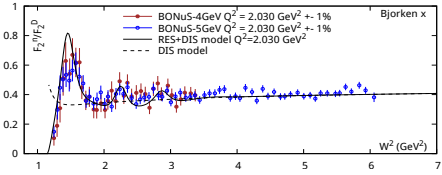
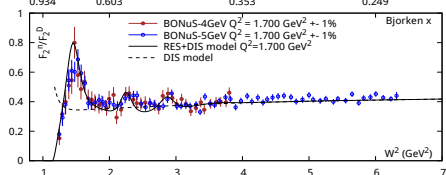
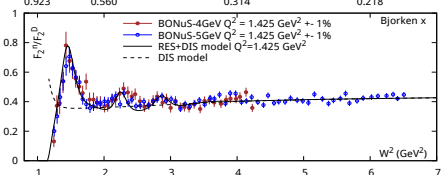
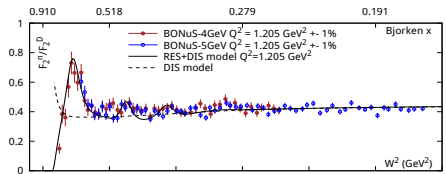
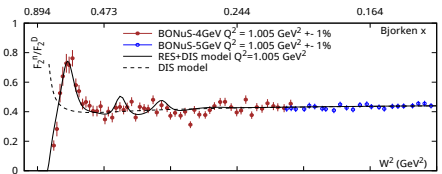
$$F_2^{n(\text{RES})} = R_{np} \left( F_2^{p(\text{RES})} - F_2^\Delta \right) + F_2^\Delta$$

# Performance of the model vs. proton and deuteron data

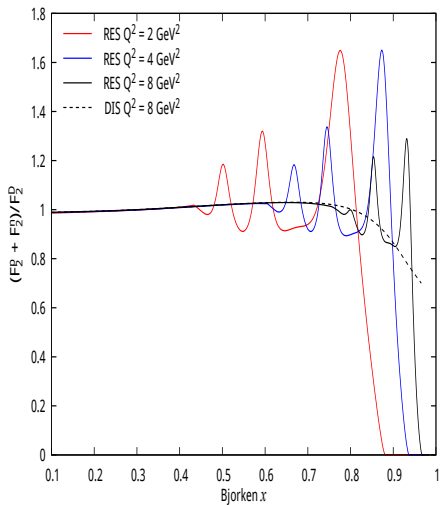
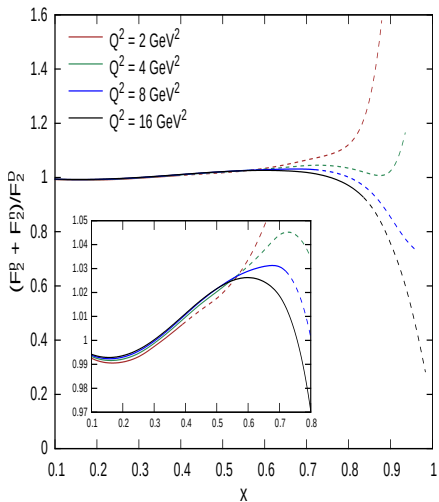


Proton and deuteron  $F_2$  computed at  $Q^2 = 1.025, 1.275, 2.525, 3.525 \text{ GeV}^2$  in a combined RES-DIS model. Data from SLAC [Whitlow,1991](#) and JLab-CLAS [Osipenko,2003,2005](#) and [NMC,1997](#).

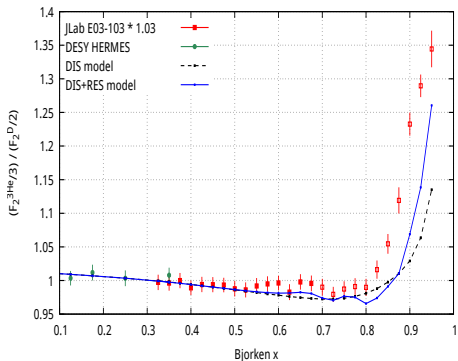
# Comparison with BONuS data $F_2^n / F_2^D$



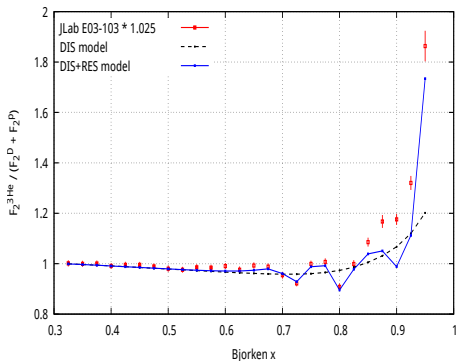
# $(F_2^p + F_2^n)/F_2^D$ in the DIS and RES models



## Comparison with $^3\text{He}$ from JLab E03103 experiment



$F_2^{3\text{He}}/F_2^D$  from JLab *Seely et al, 2009* and HERMES measurement (both corrected for the proton excess) compared with model predictions. The dashed line is DIS model, the solid line is a combined DIS+RES model.



The isoscalar ratio  $F_2^{3\text{He}}/(F_2^D + F_2^P)$  from *Seely et al, 2009* (*D.Gaskell, private communication*) compared with our predictions. The notations are similar to those of the left panel.

## Summary

- ▶ The data on the ratio of nuclear structure functions  $F_2^A/F_2^B$  (nuclear EMC effect) show nontrivial oscillating shape spanning different kinematical regions of Bjorken  $x$ .
- ▶ The data in the DIS region can be understood if we address a number of corrections including nuclear momentum distribution and binding effects, off-shell correction, meson-exchange currents as well as the matter propagation effects of hadronic component of virtual photon. Those nuclear effects result in the corrections relevant in different regions of  $x$ .
- ▶ In the resonance region (low  $Q^2$  and/or large  $x$ ) the nuclear ratios for light nuclei (2H, 3He and 3H) show a strong  $Q^2$ - and  $x$ -dependence. Current data on those ratios (JLab) can be understood in terms of smearing of the resonance structures with nuclear spectral function (the wave function in the deuteron case) except for a region of a very large  $x$  close to  $\Delta(1232)$ .



# Extras

# Table of $\chi^2$ values for all nuclei

Targets	$\chi^2/\text{DOF}$						
	NMC	EMC	E139	E140	BCDMS	E665	HERMES
$^4\text{He}/^2\text{H}$	10.8/17		6.2/21				
$^7\text{Li}/^2\text{H}$	28.6/17						
$^9\text{Be}/^2\text{H}$			12.3/21				
$^{12}\text{C}/^2\text{H}$	14.6/17		13.0/17				
$^9\text{Be}/^{12}\text{C}$	5.3/15						
$^{12}\text{C}/^7\text{Li}$	41.0/24						
$^{14}\text{N}/^2\text{H}$							9.8/12
$^{27}\text{Al}/^2\text{H}$			14.8/21				
$^{27}\text{Al}/^{12}\text{C}$	5.7/15						
$^{40}\text{Ca}/^2\text{H}$	27.2/16		14.3/17				
$^{40}\text{Ca}/^7\text{Li}$	35.6/24						
$^{40}\text{Ca}/^{12}\text{C}$	31.8/24					1.0/5	
$^{56}\text{Fe}/^2\text{H}$			18.4/23	4.5/8	14.8/10		
$^{56}\text{Fe}/^{12}\text{C}$	10.3/15						
$^{63}\text{Cu}/^2\text{H}$		7.8/10					
$^{84}\text{Kr}/^2\text{H}$							4.9/12
$^{108}\text{Ag}/^2\text{H}$			14.9/17				
$^{119}\text{Sn}/^{12}\text{C}$	94.9/161						
$^{197}\text{Au}/^2\text{H}$			18.2/21	2.4/1			
$^{207}\text{Pb}/^2\text{H}$						5.0/5	
$^{207}\text{Pb}/^{12}\text{C}$	6.1/15					0.2/5	

Values of  $\chi^2/\text{DOF}$  between different data sets with  $Q^2 \geq 1 \text{ GeV}^2$  and the predictions of KP model [NPA765\(2006\)126](#); [PRC82\(2010\)054614](#). The sum over all data results in  $\chi^2/\text{DOF} = 466.6/586$ .

## Sketch of the mean-field picture

In the the mean-field model the bound states of  $A - 1$  nucleus are described by the one-particle wave functions  $\phi_\lambda$  of the energy levels  $\lambda$ . The spectral function is given by the sum over the occupied levels with the occupied number  $n_\lambda$ :

$$\mathcal{P}_{\text{MF}}(\varepsilon, \mathbf{p}) = \sum_{\lambda < \lambda_F} n_\lambda |\phi_\lambda(\mathbf{p})|^2 \delta(\varepsilon - \varepsilon_\lambda)$$

- ▶ Due to interaction effects the  $\delta$ -peaks corresponding to the single-particle levels acquire a finite width (fragmentation of deep-hole states).
- ▶ High-energy and high-momentum components of nuclear spectrum can not be described in the mean-field model and driven by short-range nucleon-nucleon correlation effects in the nuclear ground state as witnessed by numerous studies.

## High-momentum part

- ▶ As nuclear excitation energy becomes higher the mean-field model becomes less accurate. High-energy and high-momentum components of nuclear spectrum can not be described in the mean-field model and driven by correlation effects in nuclear ground state as witnessed by numerous studies.
- ▶ The corresponding contribution to the spectral function is driven by  $(A - 1)^*$  excited states with one or more nucleons in the continuum. Assuming the dominance of configurations with a correlated nucleon-nucleon pair and remaining  $A - 2$  nucleons moving with low center-of-mass momentum we have

$$|A-1, -\mathbf{p}\rangle \approx \psi^\dagger(\mathbf{p}_1)|(A-2)^*, \mathbf{p}_2\rangle \delta(\mathbf{p}_1 + \mathbf{p}_2 + \mathbf{p}).$$

The matrix element can thus be given in terms of the wave function of the nucleon-nucleon pair embedded into nuclear environment. We assume factorization into relative and center-of-mass motion of the pair

$$\langle (A-2)^*, \mathbf{p}_2 | \psi(\mathbf{p}_1)\psi(\mathbf{p}) | A \rangle \approx C_2 \psi_{\text{rel}}(\mathbf{k}) \psi_{\text{CM}}^{A-2}(\mathbf{p}_{\text{CM}}) \delta(\mathbf{p}_1 + \mathbf{p}_2 + \mathbf{p}),$$

where  $\psi_{\text{rel}}$  is the wave function of the relative motion in the nucleon-nucleon pair with relative momentum  $\mathbf{k} = (\mathbf{p} - \mathbf{p}_1)/2$  and  $\psi_{\text{CM}}$  is the wave function of center-of-mass (CM) motion of the pair in the field of  $A-2$  nucleons,  $\mathbf{p}_{\text{CM}} = \mathbf{p}_1 + \mathbf{p}$ . The factor  $C_2$  describes the weight of the two-nucleon correlated part in the full spectral function.

$$\mathcal{P}_{\text{cor}}(\varepsilon, \mathbf{p}) \approx n_{\text{cor}}(\mathbf{p}) \left\langle \delta \left( \varepsilon + \frac{(\mathbf{p} + \mathbf{p}_{A-2})^2}{2M} + E_{A-2} - E_A \right) \right\rangle_{A-2}$$

## Average separation and kinetic energies

Average separation  $\langle \varepsilon \rangle$  and kinetic  $\langle T \rangle$  energies are related by the Koltun sum rule (exact relation for nonrelativistic system with two-body forces)

$$\langle \varepsilon \rangle + \langle T \rangle = 2\varepsilon_B,$$

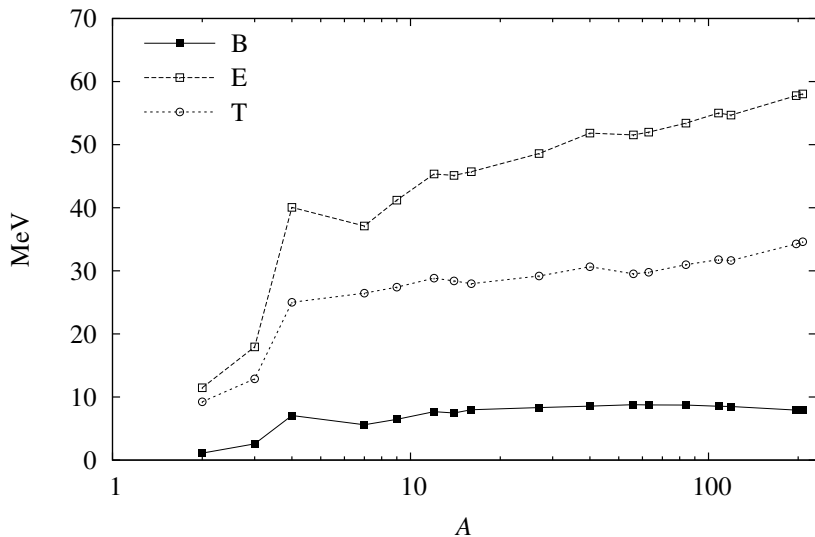
where  $\varepsilon_B = E_0^A/A$  is nuclear binding energy per bound nucleon

$$\langle \varepsilon \rangle = A^{-1} \int [dp] \mathcal{P}(\varepsilon, \mathbf{p}) \varepsilon,$$

$$\langle T \rangle = A^{-1} \int [dp] \mathcal{P}(\varepsilon, \mathbf{p}) \frac{\mathbf{p}^2}{2M}.$$

# Nuclear binding, separation and kinetic energies

Nuclear energies



# The two-component model of the spectral function

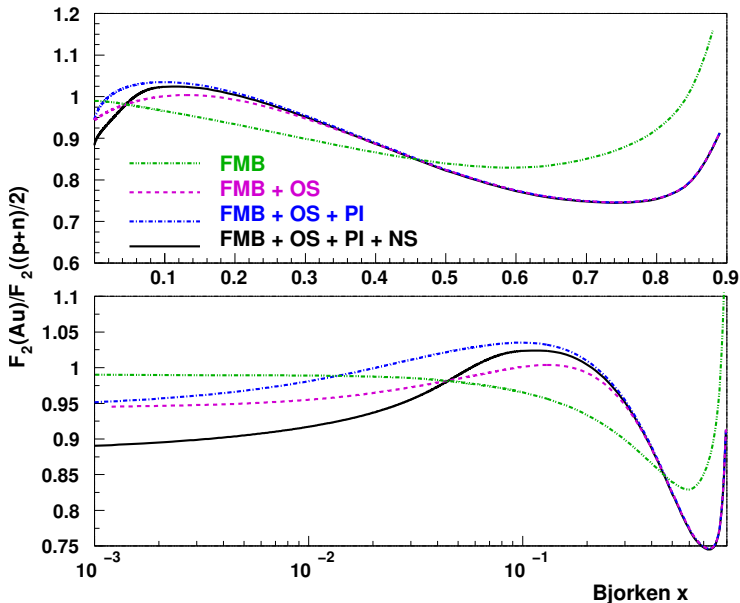
In what follows we combine the mean-field together with SRC contributions and consider a two-component model *Ciofi degli Atti & Simula, 1995 S.K. & Sidorov, 2000 S.K. & Petti, 2004*

$$\mathcal{P} = \mathcal{P}_{\text{MF}} + \mathcal{P}_{\text{cor}}$$

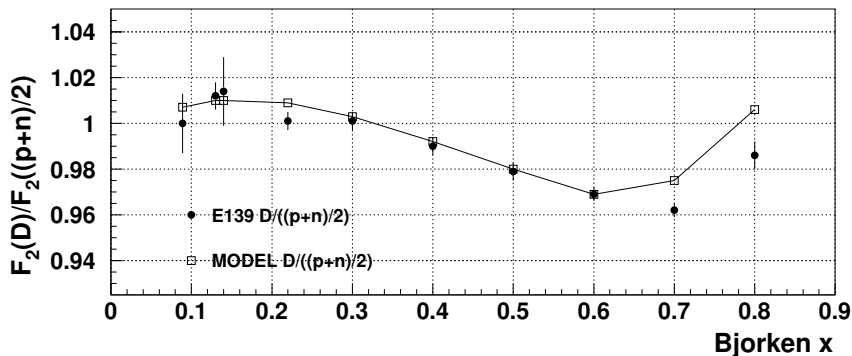
We assume that the normalization is shared between the MF and the correlated parts as 0.8 to 0.2 for the nuclei  $A \geq 4$  [for  $^{208}\text{Pb}$  0.75 to 0.25] following the observations on occupation of deeply-bound proton levels *NIKHEF 1990s, 2001*.



# Different nuclear corrections for $^{197}\text{Au}$ at $Q^2 = 10 \text{ GeV}^2$

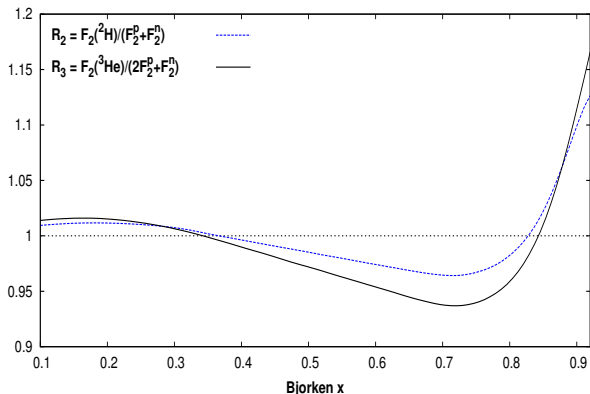


## SLAC E139 Deuteron



Model predictions (curve with open squares) in comparison with the E139 data [Gomez et al., 1994](#). Note that the E139 data points are obtained by extrapolation to  $A = 2$  using the nuclear density model [Frankfurt & Strikman, 1990](#).

## Comparison predictions for $D/(p+n)$ and ${}^3\text{He}/(2p+n)$

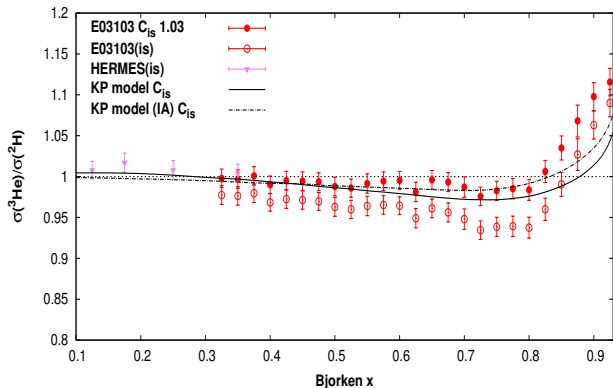


$R_2$  and  $R_3$  were calculated in the DIS model at the values of  $x$  and  $Q^2$  of JLab E03-103 experiment for  $x > 0.3$  and at fixed  $Q^2 = 3 \text{ GeV}^2$  for  $x < 0.3$ .

The Paris wave function was used for the deuteron, and the Hannover spectral function was used for  ${}^3\text{He}$ .

- ▶  $R_2$  and  $R_3$  are similar in shape. A dip at  $x \sim 0.7$  is somewhat bigger for  $R_3$  because of stronger nuclear binding in  ${}^3\text{He}$ .
- ▶ Nuclear effects cancel at  $x \approx 0.35$ , which is consistent with the measurement of EMC effect in other nuclei.

# Comparison ${}^3\text{He}/\text{D}$ with HERMES and JLab E03-103 data



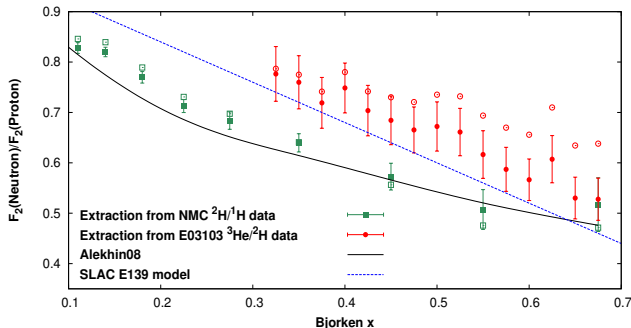
To correct for proton excess, HERMES applies the factor

$$C_{is} = \frac{AF_2^N}{ZF_2^p + NF_2^n}$$

with  $F_2^n/F_2^p$  from NMC. The E03-103 experiment does it differently, however correction factors are known.

- ▶ An unbiased way would be to compare uncorrected data, or corrected in a similar way. However, HERMES exact correction factors are not available. We uncorrect E03-103 data and then apply  $C_{is}$  together with the factor 1.03.
- ▶ After renormalization, E03-103 and HERMES data agree at the overlap ( $x = 0.35$ ). Also our predictions are in a good agreement with both data (except the region  $x > 0.8$ ).

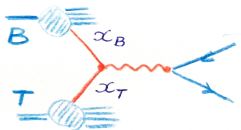
## Extraction of $F_2^n/F_2^p$ from ${}^3\text{He}/\text{D}$ vs. $\text{D}/\text{p}$



Extraction of  $F_2^n/F_2^p$  with the full treatment of nuclear effect (full symbols) and also with no nuclear effects ( $R_2 = R_3 = 1$ , open symbols).

- ▶ Significant mismatch in  $F_2^n/F_2^p$  extracted from different experiments. At  $x \sim 0.35$ , where nuclear corrections are negligible, the  $F_2^n/F_2^p$  from E03-103 is 15% higher than that from NMC.
- ▶ Normalization of  $F_2^n/F_2^p$  is directly related to normalization of  ${}^3\text{He}/\text{D}$ . Requiring  $F_2^n/F_2^p$  from E03-103 match NMC, we obtain a renormalization factor of  $1.03^{+0.006}_{-0.008}$  for  ${}^3\text{He}/\text{D}$  data.

## Drell-Yan reaction



Production of a lepton pair in hadron collision  
 $B + T \rightarrow \mu^+ \mu^- + \dots$  through the Drell-Yan mechanism:

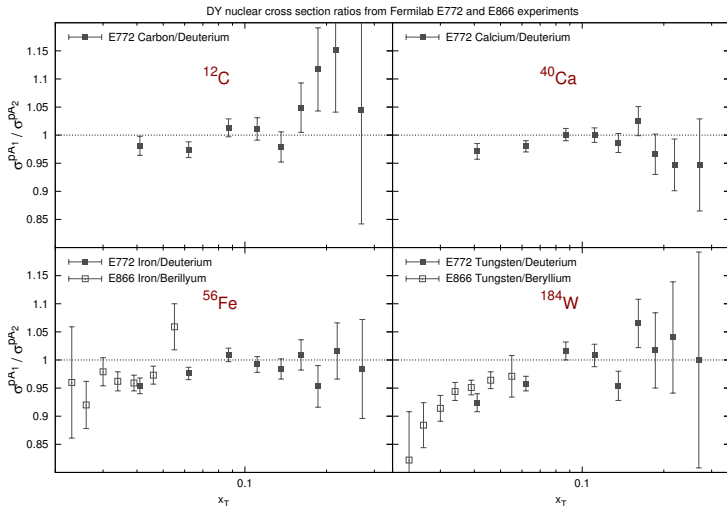
$$\frac{d^2\sigma}{dx_B dx_T} = \frac{4\pi\alpha^2}{9Q^2} K \sum_a e_a^2 \left[ q_a^B(x_B, Q^2) \bar{q}_a^T(x_T, Q^2) + \bar{q}_a^B(x_B, Q^2) q_a^T(x_T, Q^2) \right]$$

- ▶  $Q^2 = s x_T x_B$  and  $s = (p_B + p_T)^2$  the c.m. energy<sup>2</sup>.
- ▶ At small  $Q^2/s \ll 1$  and large  $x_B$  the DY process probes the target's antiquarks. For the ratios on different targets  $A_1$  and  $A_2$ :

$$\frac{\sigma_{A_1}^{\text{DY}}}{\sigma_{A_2}^{\text{DY}}} \approx \frac{\bar{q}_{A_1}(x_T)}{\bar{q}_{A_2}(x_T)}$$

# DY nuclear data from E772 and E866 experiments

Fermilab E772 and E866 experiments measure the ratio of DY yields for the DY process of 800-GeV proton with a number of targets with  $s \approx 1600 \text{ GeV}^2$  and  $4 < Q < 9 \text{ GeV}$  and  $Q > 11 \text{ GeV}$  (excluding  $J/\psi$  region).



# Drell-Yan process with nuclear targets

DY process  $p + A \rightarrow \gamma^* \rightarrow \mu^+ \mu^- + X$

Cross section is driven by

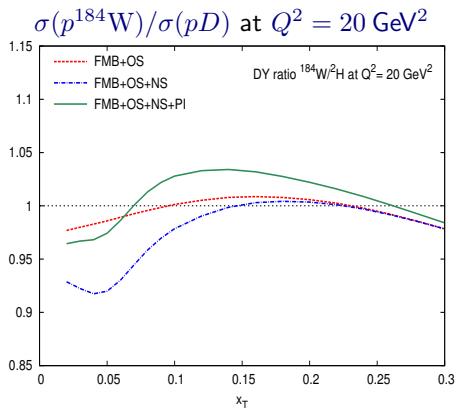
$$\sum e_q^2 [q^B(x_B)\bar{q}^T(x_T) + \bar{q}^B(x_B)q^T(x_T)]$$

In the context of Fermilab E772 & E866 experiments:

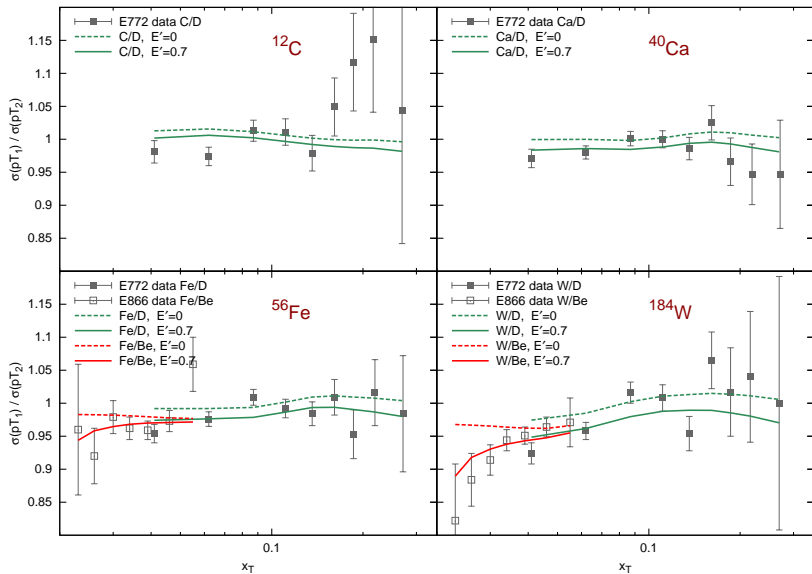
Energy  $E_p = 800$  GeV,  $s \sim 1600$  GeV<sup>2</sup>

Muon pair masses:  $4 < Q < 9$  GeV and  $Q > 11$  GeV (exclude quarkonium)

Probed region of target's Bjorken variable  $0.04 < x_T < 0.27$

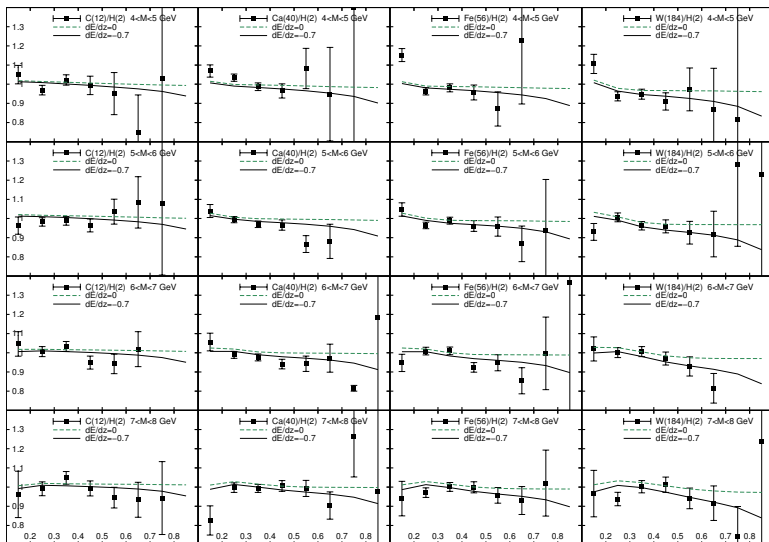






Comparison with the results of E772 & E866 Fermilab experiments *S.K. & R.Petti*,  
*PRC90(2014)045204*.

# Detailed comparison with E772 by dimuon mass bin



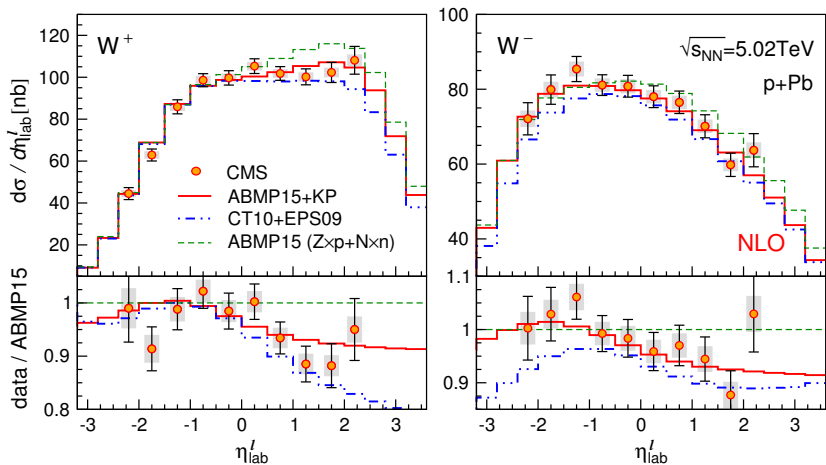
## Production of $W/Z$ in $p + Pb$ collisions at LHC

The DY mechanism of  $W/Z$  boson production in hadron/nuclear  $A + B$  collisions:

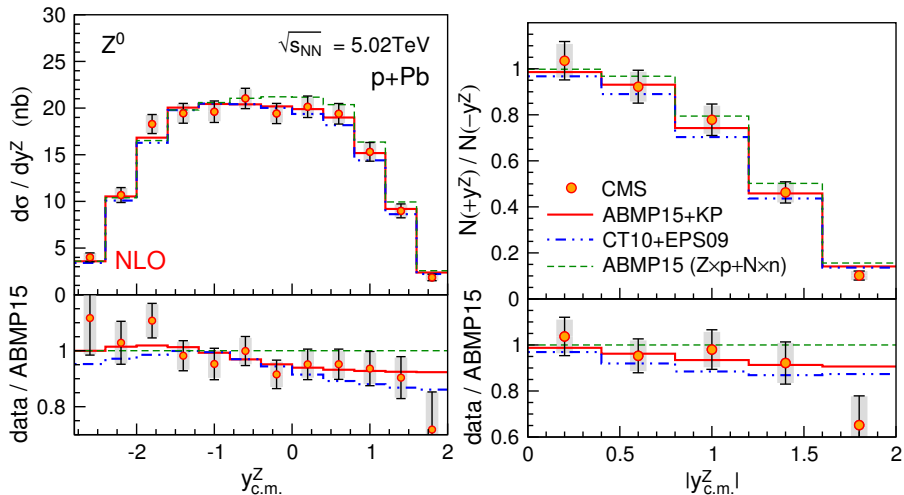
$$\frac{d^2\sigma_{AB}}{dQ^2 dy} = \sum_{a,b} \int dx_a dx_b q_{a/A}(x_a, Q^2) q_{b/B}(x_b, Q^2) \frac{d^2\hat{\sigma}_{ab}}{dQ^2 dy}$$

We study rapidity ( $y$ ) distributions of production of  $W/Z$  bosons in  $p + Pb$  collisions at LHC with  $Q^2 \sim M_Z^2$  and  $\sqrt{s} = 5.02$  TeV using KP NPDF [P.Ru, S.K., R.Petti, B-W.Zhang, arXiv:1608.06835](#).

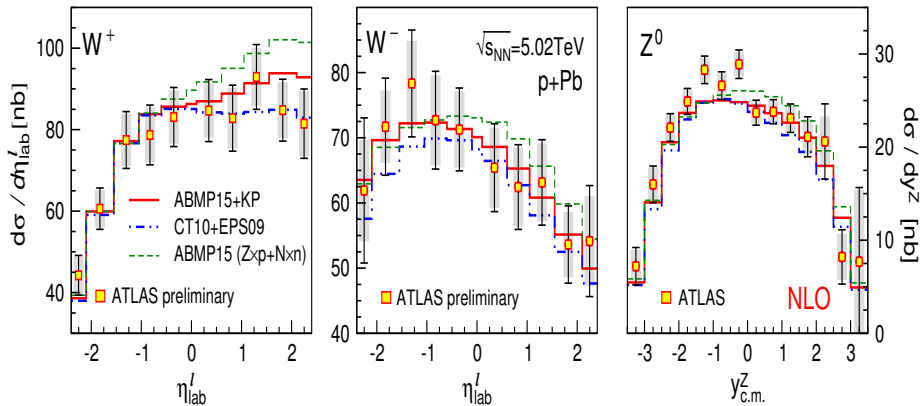
# Predictions for $W^+$ and $W^-$ and comparison with CMS data



# Predictions for $Z^0$ and comparison with CMS data



# Comparison with ATLAS data on $W/Z$ production



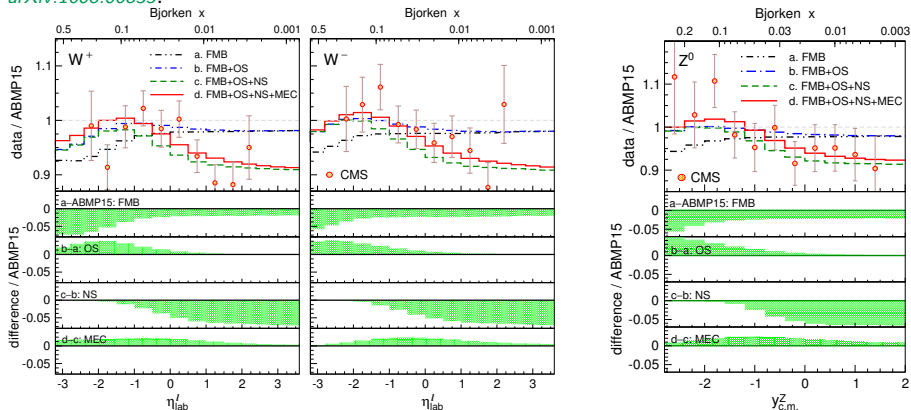
# Performance of the model in terms of $\chi^2$

Observable	$N_{\text{Data}}$	ABMP15 + KP	CT10 + EPS09	ABMP15 (Zp + Nn)
CMS experiment:				
$d\sigma^+/d\eta^l$	10	1.052	1.532	3.057
$d\sigma^-/d\eta^l$	10	0.617	1.928	1.393
$N^+(+\eta^l)/N^(-\eta^l)$	5	0.528	1.243	2.231
$N^-(+\eta^l)/N^(-\eta^l)$	5	0.813	0.953	2.595
$(N^+ - N^-)/(N^+ + N^-)$	10	0.956	1.370	1.064
$d\sigma/dy^Z$	12	0.596	0.930	1.357
$N(+y^Z)/N(-y^Z)$	5	0.936	1.096	1.785
CMS combined	57	0.786	1.332	1.833
ATLAS experiment:				
$d\sigma^+/d\eta^l$	10	0.586	0.348	1.631
$d\sigma^-/d\eta^l$	10	0.151	0.394	0.459
$d\sigma/dy^Z$	14	1.449	1.933	1.674
CMS+ATLAS combined	91	0.796	1.213	1.635

# Splitting the nuclear effects in $W/Z$ boson production

Different nuclear effects on the production cross section of  $W$  (left) and  $Z$  boson (right) in  $p + \text{Pb}$  collisions at  $\sqrt{s} = 5.02 \text{ TeV}$  *P.Ru, S.K., R.Petti, B-W.Zhang*

*arXiv:1608.06835.*



Upper axis is Bjorken  $x$  of  $\text{Pb}$  while the lower axis is (pseudo)rapidity  $(\eta)y$ .



## Nuclear effects on valence quarks vs. antiquarks

The ratios  $R_a = q_{a/A}/(Zq_{a/p} + Nq_{n/A})$  computed for the valence  $u$  and  $d$  (left) and the corresponding antiquarks (right) *S.K. & R.Petti, PRC90(2014)045204.*

